THE ASTRONOMICAL JOURNAL

VOLUME 80 January 1975 ~ No. 1428 *NUMBER 1*

Radio spectra and red shifts of 179 QSOs

John D. Kraus and Mirjana R. Gearhart
Ohio State University Radio Observatory, Columbus, Ohio
(Received 15 October 1974)

A comparison is made between radio spectral type and red shift for all known QSOs having adequate radio and optical data. A ratio of CE (centimeter excess) to N (normal) spectrum sources is defined and its variation with red shift is given. A radio color–color versus red shift diagram for the 179 QSOs is also presented. The CE/N excess is found to increase rapidly for $z > 2$ and the significance of this trend is discussed.

INTRODUCTION

QSOs may be separated by their radio spectra into two principal classes: *normal* (N) and *centimeter excess* (CE). It has been shown that this dichotomy of radio spectra relates to variability, angular size, magnitude, and polarization. Thus, Andrew *et al.* (1972) found that N-spectrum radio sources do not exhibit radio variability whereas most sources with CE spectra do. Miley (1971) has shown that for QSOs with steep N spectra there is a relationship between their overall radio size and red shift. Setti and Woltjer (1973) have found a correlation between the apparent optical magnitude and red shift for N-type QSOs. And Kronberg *et al.* (1972) have observed a correlation between the radio depolarization and red shift for a sample of QSOs with N-type radio spectra. But no analysis has been made of the CE/N ratio versus red shift. This we do for 179 QSOs.

DATA

We have endeavored to include in our study all objects for which data were available which met the following criteria:

(1) radio spectrum sufficiently well known that two indices (408–1415 MHz and 1415–6500 MHz) can be determined;
(2) accurate position available;
(3) identification made with star-like object; and
(4) optical spectral lines identified and red shift determined.

Criterion (3) eliminates any objects classified as galaxies. These commonly have N spectra and small red shifts. Eliminating the galaxies reduces the CE/N excess. Many radio sources with data meeting criteria (1) and (2) are also automatically omitted if the Palomar print fields are blank. Some of these sources may be QSOs below the plate limit; if this is due to their being red shifted out of the visible range they could have red shifts of 5 or more.

Data for the 179 QSOs of our study are listed in right-ascension order in Table I. The first column gives the source name and following it in parentheses the minutes of right ascension (1950). This is for convenience, since some names such as for 3C and 4C sources do not indicate right ascension. However, Parkes (P) and Ohio (O) names do. The second letter and the last two digits of an Ohio source name give the right ascension to one-hundredth of an hour. The second column gives the spectral index (α_1) for the frequency interval 408–1415 MHz and the third column the spectral index (α_2) for the frequency interval 1415–6500 MHz. The fourth column lists the spectral type as N for normal, F for flatter than normal, Iv for inverted, Ic for increasing, or P for peaked. The F, Iv, Ic, and P types all belong to the CE class. The fifth column lists the maximum emission red shift (z). The last column gives other source names. The letter prefixes to the source names refer to the surveys as follows: B, Bologna; N, NRAO; O, Ohio; P, Parkes; V, VRO; 3C, 3rd Cambridge; and 4C, 4th Cambridge. For more information regarding flux densities and positions reference may be made to the Master List

TABLE I. Radio spectral indices and red shifts of QSOs.

Source name		α_1	α_2	Type*	z	Other source names
00h						
3C2	(03m)	0.72	0.72	N	1.04	OB−007, N6, P0003−00
4C15.1	(03)	0.70	0.70	N	0.45	OB106, P0003+15, V15.00.01
3C9	(18)	1.02	1.06	N	2.01	OB129, 4C15.2
OB453	(32)	0.76	0.44	F	1.59	OA29, 4C42.1
P0038−020	(38)	0.73	0.73	N	1.18	OB−065, 4C−02.04
P0056−00	(56)	0.54	0.06	F	0.72	OB−094, 4C−00.6
P0056−17	(56)	0.96	0.96	N	2.13	
01h						
P0106+01	(06m)	0.70	−0.45	Iv	2.11	OC012, 4C01.2
OC026	(15)	0.80	0.80	N	0.67	OA57, P0115+02, 4C02.4
4C03.2	(18)	1.13	1.13	N	0.77	OC031, N68, P0118+03
P0119−04	(19)	0.42	0.42	F	1.96	OC−034, 4C−04.4
OC−038	(22)	0.17	0.17	F	1.07	OA60.2, 4C−00.1
4C25.5	(23)	0.88	1.42	N	2.36	OC240, P0123+25
3C47	(33)	0.99	0.99	N	0.43	OC256, 4C20.7, P0133+20
3C48	(34)	0.67	0.69	N	0.37	OC358, 4C32.8, N79
4C33.03	(41)	0.69	−0.15	Iv	1.46	OC368, DA58
3C54	(52)	0.85	0.85	N	1.46	OC487.4, N84, DA62
P0155−10	(55)	0.89	0.89	N	0.62	OC−192, MSH01−120
P0159−11	(59)	0.65	0.65	N	0.67	OC−199, N88, 3C57
02h						
DW0202+31	(02m)	0.12	0.04	F	1.47	B20202+31
P0202−17	(02)	0.10	0.22	F	1.74	
4C10.6	(14)	0.83	0.83	N	0.41	OD124, P0214+10
4C−01.11	(25)	0.80	0.80	N	0.69	OD−043, P0225−014
P0226−038	(26)	0.61	0.22	F	2.06	OD−044, 4C−03.7
4C13.14	(29)	0.39	0.21	F	2.07	OD148, P0229+13
P0232−04	(32)	0.88	0.88	N	1.44	OD−055, 4C−04.6
P0232−02	(32)	0.70	0.70	N	1.32	OD−056, 4C−02.12
P0237−23	(37)	−0.58	0.80	P	2.23	OD−263
OD−095	(56)	0.35	0.11	F	2.00	P0256−005
03h						
P0317−02	(17m)	0.84	0.36	F	2.09	OE−030, 4C−02.15
OE355	(33)	−0.11	0.30	P	1.26	4C32.14, N140
CTA26	(37)	0.19	0.39	F	0.85	OE−063, P0336−01
P0349−14	(49)	1.17	1.17	N	0.61	N147, 3C95
P0350−07	(50)	1.00	1.00	N	0.96	OE−083, N149, 3C94
04h						
P0403−13	(03m)	0.78	0.42	F	0.57	
P0405−12	(05)	0.71	0.71	N	0.57	OF−109, MSH04−12
OF−035	(20)	−0.10	0.21	P	0.92	OA129, P0420−01
OF036	(21)	−0.24	0.36	P	0.69	P0421+019
P0424−13	(24)	0.34	−0.08	Iv	2.17	OF−141.3, N178
N190	(40)	−0.36	0.19	P	0.85	OF−067, P0440−00
05h						
3C138	(18m)	0.42	0.71	F	0.76	OG130.2, 4C16.12, P0518+16
3C147	(38)	0.55	0.82	N	0.55	OG465, 4C49.14, N221
06h						
OH471	(42m)	−0.94	0.45	P	3.40	
07h						
3C175	(10m)	1.03	1.03	N	0.77	OI117, 4C11.26, P0710+11
OI318	(11)	−0.87	0.41	P	1.62	
3C181	(25)	0.84	1.14	N	1.38	OI142, N266, P0725+14
3C184.1	(34)	0.71	0.69	N	1.02	N271

TABLE I (*continued*)

Source name		α_1	α_2	Type*	z	Other source names
07^h						
P0736+01	(36)	0.11	0.11	F	0.19	OI061
OI363	(38)	−0.36	−0.01	Ic	0.63	
3C186	(40)	1.14	1.30	N	1.06	OI368, N273, 4C38.21
P0743−67	(43)	0.40	0.40	F	0.40	
08^h						
3C191	(02^m)	1.22	0.96	N	1.95	OJ103.3, P0802+10
4C05.34	(05)	0.63	0.27	F	2.88	OJ008
3C196	(09)	0.95	0.98	N	0.87	OJ417, 4C48.22, CTA45
4C02.23	(12)	0.82	0.68	N	0.40	OJ021, P0812+02
4C37.24	(27)	0.58	0.68	N	0.91	OJ346.5, WK150
3C204	(33)	0.97	1.10	N	1.11	4C65.09
3C205	(35)	0.90	1.10	N	1.53	OJ558, 4C58.16
4C19.31	(36)	0.86	0.86	N	1.69	OJ160
P0837−12	(37)	0.93	0.93	N	0.20	OJ−162, N299
3C207	(38)	0.75	0.45	F	0.68	OJ163, 4C13.38, P0838+13
4C13.39	(43)	0.80	0.80	N	1.88	OJ171
4C09.31	(46)	1.08	0.66	N	0.37	OJ078, P0846+10
3C208	(50)	1.17	1.17	N	1.11	OJ184, 4C14.28, P0850+14
4C17.46	(56)	0.91	0.85	N	1.45	OJ194
P0859−14	(59)	0.40	0.36	F	1.33	OJ−199
09^h						
3C215	(03^m)	0.90	1.08	N	0.41	OK106, 4C16.26, P0903+16
4C01.24	(06)	0.65	0.05	F	1.02	P0906+01
OK037	(22)	−0.19	0.01	P	1.72	P0922+005
4C14.31	(22)	1.03	1.03	N	0.90	OK136, P0922+14
4C39.25	(23)	0.36	−0.76	Iv	0.70	OK340, DA267
4C11.32	(26)	1.11	1.11	N	1.75	OK142
3C220.2	(27)	0.73	0.90	N	1.16	OK345.8, 4C36.15, N322
4C02.27	(32)	1.00	1.00	N	0.66	OK055, P0932+02
4C39.27	(37)	0.54	0.16	F	0.62	OK362
OK186	(52)	0.37	0.32	F	1.47	A00952+17, V17.09.04
OK290	(54)	0.40	−0.52	Iv	0.71	V25.09.08
4C32.33	(55)	0.60	0.60	N	0.53	OK393, N342
P0957+00	(57)	0.88	0.88	N	0.91	OK096, 4C00.34
10^h						
4C13.41	(04^m)	0.73	0.73	N	0.24	OL107.7, P1004+13
4C48.28	(13)	0.80	0.73	N	0.39	OL422
OL326	(15)	0.23	−0.05	Iv	1.6	
4C19.34	(22)	0.64	0.21	F	0.83	OL136
3C243	(23)	1.37	1.37	N	1.70	OL040, 4C06.40, P1023+06
4C06.41	(38)	1.05	1.05	N	1.27	
3C245	(40)	0.72	0.60	N	1.03	OL166.6, 4C12.37, P1040+12
4C05.46	(46)	1.26	1.26	N	1.12	OL078.4
4C09.37	(47)	1.21	1.21	N	0.79	OL079.2
P1049−09	(49)	0.85	0.85	N	0.34	OL−082, N359
4C20.24	(55)	0.54	0.48	F	1.11	OL293, P1055+20
P1055+01	(55)	0.29	0.29	F	0.89	OL093, DA293
OL492	(55)	0.89	0.89	N	2.39	5C02.56
11^h						
3C249.1	(00^m)	0.74	0.90	N	0.31	4C77.09, N363
4C16.30	(04)	0.57	0.57	N	0.63	OM109
3C254	(11)	0.90	1.12	N	0.73	V40.11.01
4C12.39	(16)	0.77	0.34	F	2.12	OM127, P1116+12, DA229
P1116−46	(16)	0.82	0.17	F	0.71	
P1127−14	(27)	−0.03	−0.03	Ic	1.19	OM−146, DW1127−14
4C10.33	(30)	0.74	0.74	N	0.54	OM150

TABLE I (*continued*)

Source name		α_1	α_2	Type*	z	Other source names
11^h						
3C261	(32)	0.73	1.07	N	0.61	OM356, 4C30.22, N378
P1136−13	(36)	0.81	0.50	N	0.55	OM−161
3C263	(37)	0.83	0.83	N	0.65	4C66.13, N381
P1148−00	(48)	−0.05	0.40	P	1.98	OM−080, 4C−00.47
4C49.22	(51)	0.67	−0.02	Iv	0.33	OM484
4C31.38	(54)	0.47	0.83	F	1.56	OM389, N389
4C29.45	(56)	0.16	0.16	F	0.73	OM295, CTD77
12^h						
3C268.4	(07^m)	0.92	0.92	N	1.40	ON411, 4C43.23, N393
4C13.46	(11)	0.40	0.50	F	1.14	ON119
P1217+02	(17)	0.66	0.35	F	0.24	ON029
3C270.1	(18)	0.88	0.88	N	1.52	ON330, 4C33.29, N396
4C21.35	(22)	0.66	0.66	N	0.44	ON238, P1222+21
4C25.40	(23)	1.22	0.16	F	0.27	ON239, V25.12.02
3C273	(26)	0.34	−0.02	Iv	0.16	ON044, 4C02.32, N400
P1229−02	(29)	0.61	0.53	N	0.39	ON−049, 4C−02.55
P1233−24	(33^m)	0.82	0.82	N	0.36	MSH12−207, B11232−24
3C275.1	(41)	0.96	0.90	N	0.56	ON169, 4C16.34, P1241+16
3C277.1	(50)	0.61	0.78	N	0.32	OB584, 4C56.20, N409
P1252+11	(52)	0.69	0.14	F	0.87	ON187
3C279	(53)	0.20	−0.15	Iv	0.54	ON−089, 4C−05.55
3C280.1	(58)	1.09	1.09	N	1.66	4C40.32, N417, V12.40.02
13^h						
3C281	(05^m)	0.91	0.91	N	0.60	OP009, 4C06.45
P1317−00	(17)	0.84	0.83	N	0.89	4C−00.50
4C11.45	(18)	0.71	0.71	N	2.17	OP131, P1318+11
P1327−21	(27)	0.79	0.79	N	0.53	OP−246
3C286	(28)	0.33	0.33	F	0.85	OP348, 4C30.26, N425
3C287	(28)	0.42	0.65	F	1.06	OP247, 4C25.43, N424
4C55.27	(32)	0.97	0.88	N	0.25	OP554
P1335−06	(35)	0.93	0.93	N	0.63	OP−059, 4C−06.35
3C288.1	(40)	0.89	1.07	N	0.96	OP668, 4C60.18
4C19.44	(54)	0.61	0.32	F	0.72	OP191, P1354+19, V19.13.06
P1355−41	(55)	0.80	0.72	N	0.31	MSH13−405
14^h						
3C298	(16^m)	1.18	0.95	N	1.44	OQ027.7, P1416+06, 4C06.49
4C20.33	(22)	0.57	0.57	N	0.87	OQ235, P1422+20
OQ172	(42)	−0.17	0.50	P	3.53	
P1449−012	(49)	0.63	0.63	N	1.31	OQ−081, 4C−00.57
P1453−10	(53)	0.77	0.77	N	0.94	OQ−190, DW1453−10
P1454−06	(54)	0.70	0.70	N	1.25	OQ−090, 4C−05.82
3C309.1	(59)	0.56	0.56	N	0.91	4C71.15
15^h						
OR103	(01^m)	−0.18	−0.46	Ic	1.80	
4C60.19	(02)	0.49	0.49	F	1.02	OR605, N467
P1508−05	(08)	0.62	0.62	N	1.12	OR−015, 4C−05.64
P1510−08	(10)	−0.10	−0.10	Ic	0.36	
4C37.43	(12)	0.78	0.78	N	0.37	OR321
3C323.1	(45)	0.72	0.74	N	0.26	OR276, 4C21.45, N483
P1546+027	(46)	−0.19	−0.19	Ic	0.41	
16^h						
DA406	(11^m)	0.09	0.09	F	1.40	OS319
3C334	(18)	0.93	0.93	N	0.56	OS131, 4C17.68, N500
3C336	(22)	0.73	1.00	N	0.93	OS328, 4C23.43, N501
4C26.49	(34)	0.72	0.72	N	0.56	OS257, P1634+26
3C345	(41)	0.26	−0.19	Iv	0.60	OS368, 4C39.48, N513

TABLE I (*continued*)

Source name		α_1	α_2	Type*	z	Other source names
17^h						
3C351	(04^m)	0.73	0.83	N	0.37	4C60.24
18^h						
P1801+01	(01^m)	1.10	0.72	N	1.52	DW1801+01
3C380	(28)	0.75	0.52	N	0.69	OU447, 4C48.46, N565
19^h						
OV591	(54^m)	0.12	0.00	F	1.22	
20^h						
P2005−04	(05^m)	1.11	0.57	N	0.59	3C407
P2059+034	(59)	−0.15	−0.15	Ic	0.37	OW098
21^h						
P2115−30	(15^m)	0.72	0.74	N	0.98	OX−325, MSH21−34
3C432	(20)	0.98	1.21	N	1.81	OX134.2, 4C16.72
P2128−12	(28)	−0.15	−0.09	Ic	0.50	
P2134+004	(34)	−1.06	−0.81	Ic	1.94	OX057
P2135−14	(35)	0.86	0.77	N	0.20	OX−158
OX161	(36)	−0.03	0.10	P	2.42	
P2144−17	(44)	0.63	0.63	N	0.68	OX−175
4C06.69	(45)	0.05	−0.26	Iv	0.37	OX076.1, P2145+06
P2146−13	(46)	1.00	1.00	N	1.80	OX−178
22^h						
P2216−03	(16^m)	0.86	−0.37	Iv	0.90	OY−072, 4C−03.79
3C446	(23)	0.50	0.12	F	1.40	OY−039, P2223−05, N687
CTA102	(30)	0.06	0.35	F	1.04	OY150, 4C11.69, P2230+11
3C454	(49)	0.70	0.80	N	1.76	4C18.67, P2249+18, N699
4C15.76	(51)	0.08	0.08	F	0.86	OY185, P2251+15, N701
4C11.72	(51)	0.77	0.77	N	0.32	OY186, P2251+11
3C455	(52)	0.78	0.98	N	0.54	OY188, 4C12.79, P2252+12
OY091.3	(54)	−0.03	−0.35	Ic	2.09	P2254+024
23^h						
4C29.68	(25^m)	0.92	0.65	N	1.02	OZ243, B22325+29
P2340−036	(40)	0.70	0.70	N	0.90	
4C09.74	(44)	0.15	0.30	F	0.68	OZ073.5, P2344+09
P2345−16	(45)	0.35	−0.23	Iv	0.60	OZ−176
P2353−68	(53)	0.24	0.67	F	1.72	
4C14.85	(54)	0.75	1.05	N	1.81	OZ191, P2354+14

* N (normal), F (flatter-than-normal), Iv (inverted), Ic (increasing), P (peaked).

of Radio Sources (Dixon 1970) and to the seven installments of the Ohio survey.

The spectral indices are defined by $\alpha_1 = \log(S_{408}/S_{1415})/\log(1415/408)$ and $\alpha_2 = \log(S_{1415}/S_{6500})/\log(6500/1415)$. The choice of the three frequencies 408, 1415, and 6500 MHz was dictated by practical considerations. A flux density at 1415 MHz is available from the Ohio survey for nearly all of the sources, while flux densities for many sources are available at 408 MHz from the Parkes (Ekers 1969) and other surveys. Flux densities at 6500 MHz have been measured at the Algonquin Radio Observatory for sources in the Ohio Spectral Lists and also many other sources. In many cases flux densities were not available at either 408 or 6500 MHz but at somewhat higher or lower frequencies and in these cases the flux densities at 408 or 6500 MHz were either interpolated or extrapolated. The lists of Kellermann *et al.* (1969) and Kellermann and Pauliny-Toth (1973) were used for many of the 3C sources. In a similar way the lists of Shimmins *et al.* (1969) and Wall (1972) were used for Parkes sources. Flux densities from Medd *et al.* (1972) were also employed particularly on variable sources where a median recent-epoch flux density was chosen. Although variability affects the index (α_2) there are no cases where it changes the spectral type. A number of flux densities at 6500 MHz were kindly provided from unpublished measurements by Morley Bell of the National Research Council, Canada.

Some CE sources have such complex radio spectra that more than two indices are needed to describe the spectrum. Although more indices may be desirable, we have limited our study to two indices which are, in any case, far more adequate than a single index.

The red-shift data were obtained from a number of sources: Arp *et al.* (1972), Burbidge and Burbidge (1969), Burbidge and O'Dell (1972), Bolton *et al.* (1968), Burbidge and Strittmatter (1972), Bell and Fort (1973), Carswell and Strittmatter (1973), DeVeny *et al.* (1971), Lynds and Wills (1972), Medd *et al.* (1972), Peterson and Bolton (1972), Schmidt and Matthews (1964), Tritton (1971), and Wampler *et al.* (1973).

The data of Table I are presented by the radio color–color versus red-shift diagram of Fig. 1. The 408–1415-MHz index (α_1) is plotted as abscissa and the 1415–6500-MHz index (α_2) plotted as ordinate while the red shifts are shown by circles of different

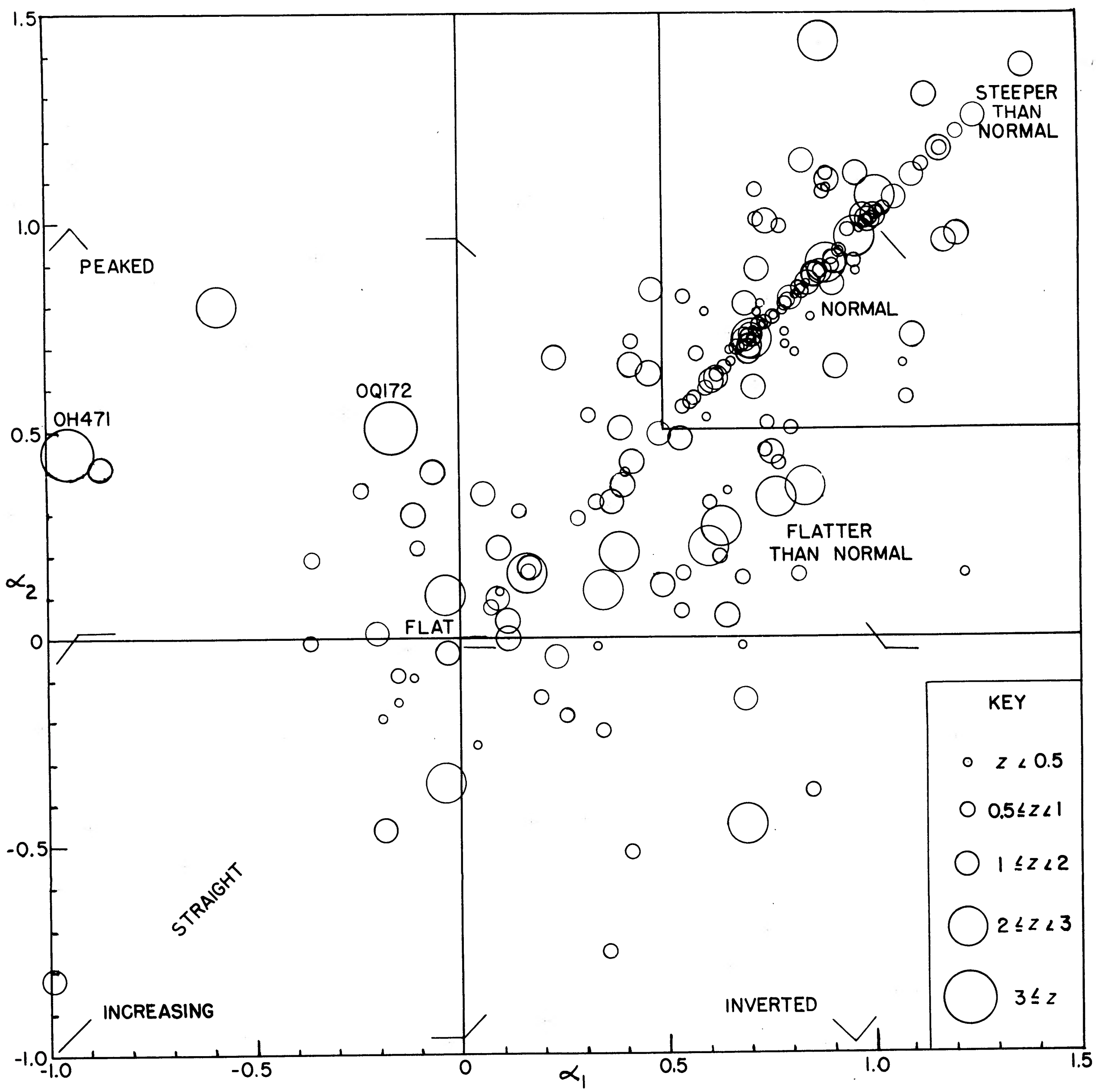

FIG. 1. Radio spectral index versus red shift for 179 QSOs. The abscissa gives the index (α_1) for the frequency interval 408–1415 MHz and the ordinate the index (α_2) for the interval 1415–6500 MHz. The red shift is indicated by the circle size (see key at lower right). Normal and steeper-than-normal spectrum sources are at the upper right, peaked at upper left, inverted at lower right, and increasing at lower left. Flat-spectrum sources are at the middle of the diagram near $\alpha_1=\alpha_2=0$. All sources for which either or both α_1 and α_2 are less than 0.5 are classified as centimeter excess (CE) sources.

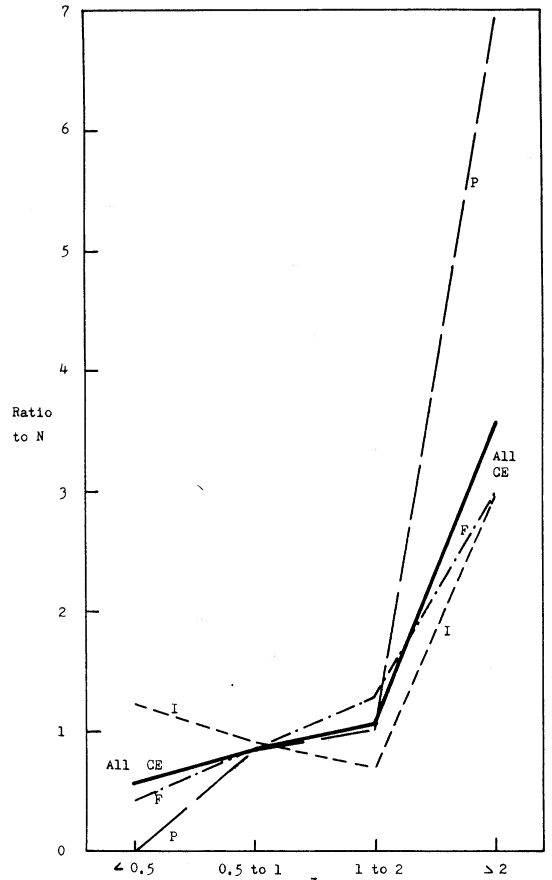

FIG. 2. Percentage ratio of QSOs of various CE types to N as a function of red-shift increment from Table II. See Table II footnote for meaning of symbols.

sizes divided into five categories: $0.5<z$, $0.5\leq z<1.0$, $1\leq z<2$, $2\leq z<3$, and $3\leq z$ (see key at lower right of Fig. 1). Shapes of the radio spectra at different parts of the diagram are suggested by the two-segment lines located around the edges of the diagram. The normal and steeper-than-normal spectrum sources occupy the upper right of the diagram, the peaked spectrum sources the upper-left quadrant, and the increasing and inverted spectrum sources the lower-left and lower-right quadrants, respectively. The flatter-than-normal spectrum sources occupy the part of the upper-right quadrant not included in the normal or steeper-than-normal part. The normal and steeper-than-normal spectrum QSOs are classified as N and the remainder as CE sources. The indices for all normal or steeper-than-normal sources are both greater than 0.5. These definitions are arbitrary but convenient and follow closely (although not exactly) the definitions given originally by Andrew *et al.* (1972).

The radio spectra of the high-red-shift QSOs OH471 ($z=3.40$) and OQ172 ($z=3.53$) are complex with two peaks and a low-frequency cutoff (Gearhart *et al.* 1974). It is significant that these sources would remain CE types (as defined herein) for red shifts of 0–5 or more.

The clustering of many sources along the main diagonal (from lower left to upper right) is an indication of the tendency for many sources to exhibit a simple power-law (straight) spectrum in the frequency range being investigated. This tendency is particularly strong among the normal-spectrum sources.

DISCUSSION

The results are summarized in Table II and the trends displayed in Fig. 2. The CE/N excess is small at red shifts below 2 but increases sharply for $z>2$. There is over three times the probability of a red shift greater than 2 for a QSO with a CE instead of an N spectrum. This probability is raised to seven times if the spectrum is peaked; however, the statistics in this case suffer from small numbers. Conversely, there is twice the probability of a red shift less than 0.5 if the source has an N instead of CE spectrum. The trend could be explained as indicating that CE QSOs are intrinsically more luminous than N ones but whether such a causal relation is responsible is not clear because (1) the sample is not complete; (2) the correlation found by Setti and Woltjer suggests that the deficit of high-red-shift N QSOs could be ascribed to optical faintness; and (3) Strittmatter *et al.* (1974) indicate that color selection

TABLE II.* Numbers and percentages of QSOs of different spectral types.

Red shift	N	N%	I	I%	F	F%	P	P%	All CE	All CE%	CE/N
$z<0.5$	23	22	6	27	4	10	0	0	10	13	0.58
$0.5\leq z<1$	41	40	8	36	15	34	3	27	26	34	0.85
$1\leq z<2$	34	33	5	23	18	42	4	37	27	36	1.07
$2\leq z<3$	5	5	3	14	6	14	2	18	11	14	3.02
$3\leq z$	0	0	0	0	0	0	2	18	2	3	∞
	103	100	22	100	43	100	11	100	76	100	

* N (normal), I (inverted and increasing), F (flatter than normal), P (peaked), CE (centimeter excess).

has operated against finding high-z QSOs, such as OH471 with a neutral optical spectrum, but no conclusion is drawn regarding CE versus N types. It is of interest that Baldwin *et al.* (1974) have found 175 absorption lines, mostly shortward of Lyman α for OQ172 ($z=3.53$).

Although the net result of the above effects cannot yet be determined quantitatively, the CE/N excess found is significant in the sense that it reflects completely the present state of the observational data.

ACKNOWLEDGMENTS

The Ohio State University Radio Observatory is administered by the Electrical Engineering Department in cooperation with the Astronomy Department of the Ohio State University. We appreciate the use of the 150-ft (46-m) telescope at the Algonquin Radio Observatory of the National Research Council, Canada, and the assistance of B. H. Andrew and others of its staff for obtaining many of the short-wavelength flux densities. We are indebted to the following for communicating red shifts prior to publication: Eric Craine (OL326), E. J. Wampler (OV591 and OX161), and D. Wills (OR103).

REFERENCES

Andrew, B. H., Medd, W. J., Harvey, G. A., and Locke, J. L. (1972). Nature **236**, 445.
Arp, H. C., Burbidge, E. M., Mackay, C. D., and Strittmatter, P. A. (1972). Astrophys. J. Lett. **171**, L41.
Baldwin, J. A., Burbidge, E. M., Burbidge, G. R., Hazard, C., Robinson, L. B., and Wampler, E. J. (1974). Astrophys. J. **193**, 513.
Bell, M. B., and Fort, D. N. (1973). Astrophys. J. **186**, 1.
Bolton, J. G., and Wall, J. V. (1970). Aust. J. Phys. **23**, 789.
Bolton, J. G., Kinman, T. D., and Wall, J. V. (1968). Astrophys. J. Lett. **154**, L105.
Burbidge, G. R., and Burbidge, E. M. (1969). Nature **222**, 735.
Burbidge, G. R., and O'Dell, S. L. (1972). Astrophys. J. **178**, 583.
Burbidge, E. M., and Strittmatter, P. A. (1972). Astrophys. J. Lett. **172**, L37.
Carswell, R. F., and Strittmatter, P. A. (1973). Nature **242**, 394.
DeVeny, J. B., Osburn, W. H., and Janes, K. (1971). Publ. Astron. Soc. Poc. **83**, 611.
Dixon, R. S. (1970). Astrophys. J. Suppl. Series 20, No. 180.
Ekers, J. A., Ed. (1969). Aust. J. Phys. Astrophys. Suppl. No. 7.
Gearhart, M. R., Kraus, J. D., Andrew, B. H., Blake, G., Scott, P., Ryle, M., Braude, S. Ya., Sharykin, N. K., Zhouck, I. N., Bridle, A. H., Conklin, E. K., Douglas, J. N., Hachenberg, O., Thiel, M., Kaufmann, P., Purton, C. R., Feldman, P. A., Marsh, K. A., Stull, M. A., Price, K., Warner, J. W., Assousa, G., and Balick, B. (1974). Nature **249**, 743.
Kellermann, K. I., Pauliny-Toth, I. I. K., and Williams, P. J. S. (1969). Astrophys. J. **157**, 1.
Kellermann, K. I., and Pauliny-Toth, I. I. K. (1973). Astron. J. **78**, 828.
Kronberg, P. P., Conway, R. G., and Gilbert, J. A. (1972). Mon. Not. R. Astron. Soc. **156**, 275.
Lynds, R., and Wills, D. (1972). Astrophys. J. **172**, 531.
Medd, W. J., Andrew, B. H., Harvey, G. A., and Locke, J. L. (1972). Mem. R. Astron. Soc. **77**, 109.
Miley, G. K. (1971). Mon. Not. R. Astron. Soc. **152**, 477.
Peterson, B. A., and Bolton, J. G. (1972). Astrophys. J. Lett. **173**, L19.
Setti, G., and Woltjer, L. (1973). Astrophys. J. Lett. **181**, L61.
Shimmins, A. J., Manchester, R. N., and Harris, B. J. (1969). Aust. J. Phys. Astrophys. Suppl. No. 8.
Schmidt, M., and Mattews, T. A. (1964). Astrophys. J. **139**, 781.
Strittmatter, P. A., Carswell, R. F., Gilbert, G., and Burbidge, E. M. (1974). Astrophys. J. **190**, 509.
Tritton, K. (1971). Mon. Not. R. Astron. Soc. **155**, 1.
Wall, J. V. (1972). Aust. J. Phys. Astrophys. Suppl. No. 24.
Wampler, E. J., Robinson, L. B., Baldwin, J. A., and Burbidge, E. M. (1973). Nature **242**, 336.